

pubs.acs.org/est Article

# Resolving Atmospheric Mercury Loading and Source Trends from Isotopic Records of Remote North American Lake Sediments

Ryan F. Lepak,\* Sarah E. Janssen, Daniel R. Engstrom, David P. Krabbenhoft, Michael T. Tate, Runsheng Yin, William F. Fitzgerald, Sonia A. Nagorski, and James P. Hurley



Cite This: Environ. Sci. Technol. 2020, 54, 9325–9333



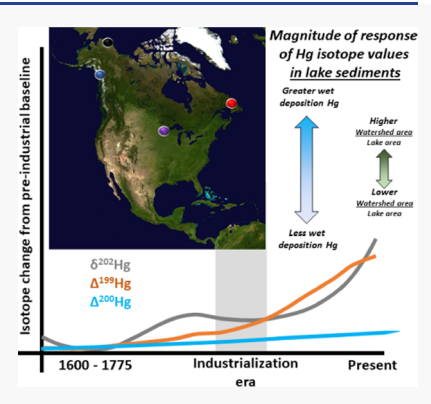
**ACCESS** 

Metrics & More



Supporting Information

ABSTRACT: The strongest evidence for anthropogenic alterations to the global mercury (Hg) cycle comes from historical records of mercury deposition preserved in lake sediments. Hg isotopes have added a new dimension to these sedimentary archives, promising additional insights into Hg source apportionment and biogeochemical processing. Presently, most interpretations of historical changes are constrained to a small number of locally contaminated ecosystems. Here, we describe changes in natural Hg isotope records from a suite of dated sediment cores collected from various remote lakes of North America. In nearly all cases, the rise in industrial-use Hg is accompanied by an increase in  $\delta^{202}$ Hg and  $\Delta^{199}$ Hg values. These trends can be attributed to large-scale industrial emission of Hg into the atmosphere and are consistent with positive  $\Delta^{199}$ Hg values measured in modern-day precipitation and modeled increases in  $\delta^{202}$ Hg values from global emission inventories. Despite similar temporal trends among cores, the baseline isotopic values vary considerably among the different study regions, likely attributable to



differences in the fractionation produced in situ as well as differing amounts of atmospherically delivered Hg. Differences among the study lakes in precipitation and watershed size provide an empirical framework for evaluating Hg isotopic signatures and global Hg cycling.

# **■** INTRODUCTION

Mercury (Hg) is a metal with a comparatively high vapor pressure and thus is susceptible to atmospheric transport and deposition in locations without direct anthropogenic influence. Reactions in the atmosphere can produce gaseous oxidized and particulate bound forms of Hg that can then undergo rapid deposition into aquatic ecosystems. Once deposited, Hg is susceptible to redox reactions, partitioning, and methylation from microbes.2 The latter is of concern because the microbially mediated formation of methylmercury,<sup>2</sup> a potent neurotoxin, can result in bioaccumulation that leads to fish that are a millionfold higher in concentration than surrounding waters.3 This can lead to deleterious health and reproductive effects in fish, fish-consuming humans, 4 and wildlife.5 The amount of actively cycling Hg has increased 3-4 times since the early 19th century, and most of that increase has been attributable to anthropogenic activity<sup>6-11</sup> (e.g., fossil fuels and mining) rather than natural sources (e.g., volcanic eruptions).

An understanding of the extent of ubiquitous contamination and important aqueous and atmospheric transformation pathways was not fully realized until the early 1990s with the application of trace metal clean techniques that allowed researchers to accurately measure Hg in the environment. For this reason, reconstruction of Hg deposition trends predating the 1990s relies on media that can accurately record

Hg deposition through time. Well-positioned, properly collected, and dated sediment <sup>13</sup> and ice cores have been shown to be the best available means for historical reconstruction. <sup>6–9,14–18</sup> It is through these media that we can better understand the extent of human alterations to the global Hg cycle, and the conditions (such as application of watershed to lake area ratios and proximity to Hg emission sources) that control the extent of Hg contamination. <sup>6–9,14–18</sup>

Mercury has seven stable isotopes that exist at varying natural abundancies. Subtle changes in the relative proportion of these isotopes (at thousandths of a percent) are environmentally diagnostic and can be measured precisely (expressed as per mille—‰). Through a combination of lab-based experiments and directly measured media, reactions that affect Hg isotope ratios can be assessed to more accurately describe the relative contribution of specific sources. Reaction processes driven by kinetics (e.g., sorption, methylation 22) and equilibrium exchange between reactant and product tend to produce shifts in the relative abundance of Hg isotopes in a

Received: January 29, 2020 Revised: June 26, 2020 Accepted: June 27, 2020 Published: June 27, 2020





manner dependent on mass.  $^{20,23,24}$  These mass-dependent fractionations (MDFs) affect all Hg isotopes but are typically denoted with a  $\delta$ , i.e.,  $\delta$   $^{202}$ Hg. Hg that undergoes reactions with light (photoreduction,  $^{23}$  photodemethylation,  $^{23,25}$  and halide oxidation  $^{26}$ ), or undergoes extensive equilibrium exchanging,  $^{27}$  can produce changes in the relative isotope abundancies that do not depend on mass.  $^{19,24}$  These mass-independent fractionations (MIFs) are typically associated with odd isotopes (denoted with a  $\Delta$ , i.e.,  $\Delta$   $^{199}$ Hg and  $\Delta$   $^{201}$ Hg) and most commonly are observed as the byproduct of photochemical demethylation (in biota) and photochemical reduction (in sediments, soil, and air) because of differences between even and odd isotope spins.  $^{20}$ 

A secondary, less prominent MIF mechanism has also been empirically characterized, with even isotopes (even-MIF) and is currently considered unrelated to photochemical reduction and photochemical demethylation.  $^{20,24,28,29}$  This fractionation process is thought to be the result of nuclear self-shielding and is common to all Hg isotopes. It is typically referred to as even-MIF, denoted as  $\Delta^{200} \rm Hg$  (and less commonly  $\Delta^{204} \rm Hg)$  because it cannot be easily observed in Hg isotopes 196, 198, 199, 201, and 202 for various reasons. While the mechanism and environmental relevance of even-MIF is of current debate, the utility of  $\Delta^{200} \rm Hg$  as a conservative tracer of the depositional pathway of gaseous elemental Hg  $^{32-35}$  (GEM) and precipitation-delivered Hg  $^{28,36}$  is agreed upon.

Ultimately, the differences in the Hg isotope values provide an opportunity to leverage three dimensions of Hg source and process-tracing to investigate how Hg contributions to atmospheric deposition have changed prior to and following industrialization with the continued inputs of anthropogenically released Hg. Using dated lake-sediment cores 7,8,40,41 from remote locations of North America that span large geographic domains, we hypothesized that with Hg isotope ratios we could estimate the relative shifts in Hg sources from the North American airshed to these lakes. These well-characterized lakes, receiving predominantly atmospherically sourced Hg (delivered via precipitation or dry deposition of GEM), also allowed us to evaluate the importance of geographic and lakespecific characteristics to the overall Hg isotope composition, the response of the isotopes to anthropogenic perturbations through time, and mechanisms likely contributing to their spatial and temporal trends.

# ■ METHODS

Study Sites. A single lake sediment core was collected from each of nine mostly remote, undisturbed lakes located in three different regions of North America: Alaska, Minnesota, and Newfoundland (Figure S1). Three of the Alaskan lakes (Sapsucker, Rectangle, Goldeneye) are in the temperate rainforest of the north Pacific coast, on northern Chichagof Island. A fourth lake (Perfect) is in the Arctic on the north slope of the Brooks Range. Two of the three Minnesota lakes (Locator and Dunnigan) are in the northern part of the state near the US/Canadian border, while the third (Square) is in a semirural area near the state's eastern border with Wisconsin. The watersheds of the two northern lakes are entirely forested, while that of Square Lake has a mixed forest and scattered agricultural watershed. Newfoundland sites (Clever, Tomtit) are near the Gulf of St. Lawrence in the forest/tundradominated western region of the province.

The physicochemical characteristics of the study sites and dates of collection are summarized in Table S1. Most lakes are

relatively small (surface area = 0.02–0.5 km²), moderately deep (maximum depth = 4.3–20.7 m), and are situated in small catchments relative to lake-surface area  $(A_c/A_l=1.2-15.1)^{.41,42}$  Annual precipitation varies considerably among the study areas, ranging from ~30 cm in arctic Alaska to ~170 cm in southeastern Alaska. Hg wet deposition is the highest in Minnesota (7.7–9.4  $\mu$ g m<sup>-2</sup> yr<sup>-1</sup>) and the lowest in the Arctic (1.5  $\mu$ g m<sup>-2</sup> yr<sup>-1</sup>—Table S1). Lake-water chloride also exhibits strong geographic variation, He highest concentrations in near-coastal sites (Newfoundland = 2.7–3.0 ppm; southeast Alaska = 1.4–1.5 ppm) and the lowest in continental sites (Arctic = 0.19 ppm, Minnesota = 0.32–0.35 ppm). The single outlier to this pattern, Square Lake (Cl<sup>-</sup> = 5.6 ppm), is affected by road-salt runoff from its developed watershed.

Core Collection and Age Dating. The cores examined here were collected between 2000 and 2015 (Table S1). Minnesota and arctic cores were obtained by piston coring methods, while those from Newfoundland and southeastern Alaska were collected by gravity corer (Pylonex HTH). Sediment age dating and total Hg profiles for all study lakes have been presented previously: Minnesota, 7,43 arctic Alaska, 40 Newfoundland, and southeastern Alaska. However, several of the lakes were recored more recently (at the same coring locations; Figure S1), and the isotope results presented here are from those newer cores: Locator, Dunnigan (2010), Square, Sapsucker, Rectangle, and Goldeneye (2015).

Sediment cores were dated by  $^{210}$ Pb using isotope-dilution,  $\alpha$  spectrometry methods, and the constant rate of supply (crs) dating model.  $^{14,44}$  The resulting activity profiles for excess  $^{210}$ Pb were effectively exponential with respect to cumulative dry mass, indicating near-constant sediment accumulation. Dates prior to the oldest explicit  $^{210}$ Pb date (typically 1800–1820) were extrapolated based on cumulative dry mass (g cm $^{-2}$ ) and the mean mass accumulation rate (g cm $^{-2}$  yr $^{-1}$ ) for each core.

Sample Preparation. Sediment samples were weighed into 40 mL borosilicate vials (<0.5 gr), aqua regia (5 mL; 3:1 HNO<sub>3</sub>:HCl -15.8 M:11.65 M) was added, and samples were allowed to sit overnight at room temperature. The samples were then digested for 8 h at 90 °C in an acid-resistant water bath within an acid-resistant hood. Following digestion, cooled solutions were diluted to 50% acid concentration and quantified for total mercury (HgT) using an adaptation of EPA method 1631.<sup>38,45,46</sup> Process blanks were consistently below the lab reported detection limits (0.04 ng L<sup>-1</sup>). A standard reference material was analyzed in 10% of the sample count (IAEA SL1, lake sediment, 130 ng g<sup>-1</sup>); recovery was  $101 \pm 4\%$ . Further, when mass availability allowed, samples were analyzed in duplicate or triplicate. Relative standard deviations were on average 6%. Samples containing more than 15 ng of Hg were run directly.<sup>38,46</sup>

A subset of samples required preconcentration prior to Hg isotope analysis because they were below our detection limits for Hg isotope analysis. The preconcentration method leverages an adaptation of U.S. Environmental Protection Agency (EPA) method 1631 that relies on gold trap amalgamation and slow thermal decomposition (45 min) into an oxidizing solution (3:1 HNO<sub>3</sub>:BrCl, 40% v/v). 45,47 Similar to previous results, 47 recovery was within 95–105% and reference materials agreed well with previous results.

**Hg Isotope Analysis.** A suitable aliquot was removed from either the direct digest or a preconcentration solution to

achieve 0.5-1.0 ng Hg mL<sup>-1</sup> solutions for isotope analysis at the USGS Mercury Research Lab (Middleton, WI). The analysis concentration was dictated by the mass of Hg present in the solution. Digests and preconcentration solutions are different matrices, and therefore the analyses were performed separately with standard sample bracketing by matrix-matched NIST 3133. The sample introduction process, lab protocols, and instrument tuning conditions are described more fully elsewhere. 38,46,47 We continue to follow the convention for expressing MDF ( $\delta$ ) and MIF ( $\Delta$ ), respectively.<sup>20,31</sup> Sample voltage was consistently within 10% of the NIST bracketing solution, and equally distributed UM-Almaden measurements in 20% of the total sample count were made to confirm instrument precision and accuracy. UM-Almaden and IAEA SL1 were consistent with previous findings.<sup>38,47</sup> The analytical variance (2 SD) for IAEA SL1 was 0.06%, 0.06%, and 0.04% for  $\delta^{202}$ Hg,  $\Delta^{199}$ Hg, and  $\Delta^{200}$ Hg, respectively, and represents the largest uncertainty for all reference standards and thus reflects the sampling uncertainty for each isotope. Data may be found in Table S2, and quality assurance results are in Table S3.42

Relative Changes in Isotope Values. To compare cores directly, each core was relativized for background differences in each isotope. Two approaches for data normalization were considered; the fractional increase (Z-score) and baseline subtraction. Statistically, the fractional increase is favorable because it is nonparametric (data response is assumed nonlinear) and works independently, thus reducing user decisions and biases. However, the output variables are reported Z-scores that accurately portray points of inflection, especially in time series, but are less intuitive for the reader because they do not reflect an isotope value. For this reason, we elected to present the baseline subtracted approach and place the Z-scores into the Supporting Information though we note that the two outputs are related. We define baseline in each isotope as the averaged isotopic value from 1600 to 1775 (with the exception of the Clever record, which began in 1812) because other work has demonstrated that industrialization and the increase in coal consumption began ca. 1800, thus this time frame predates the major global pulse of anthropogenically released Hg. 7-9,40,41 Although there were some minor changes prior to 1775 (Table S2), there were no significant trends in the isotope values. The background average specific to each core was then subtracted from the specific values of that respective core. In effect, this results in the net change in the Hg isotope values relative to baseline conditions and thus quantifies how the isotope value has changed (designated by  $\delta^{202}$ Hg<sub>EF</sub>,  $\Delta^{199}$ Hg<sub>EF</sub>, or  $\Delta^{200}$ Hg<sub>EF</sub>). All raw data of the site characteristics, Hg isotope values, associated quality assurance, and statistical evaluations may be found in the Supporting

**Data Smoothing.** To smooth the data trends, locally weighted scatterplot smoothing (LOWESS) and kernel regressions were each used. The nonuniform distribution of data with more information in more recent years led to the need for a smoothing algorithm adequately flexible to change the sampling window through time. Due to the comparatively more flexible Kernel approach, changes are described in the main manuscript using Kernel regression (500 iterations) in a manner similar to previous work, while the LOWESS outputs may be found in the Supporting Information (Figures S2–S4). Here, we chose to adhere to the smoothing parameters previously presented, and remained consistent with the

recommendations for Nadaraya-Watson estimation, flexible bandwidth window optimized by leave-one-out cross validation, and uncertainty based on refitting and resampling with bootstrapping.<sup>48</sup>

## ■ RESULTS AND DISCUSSION

**Regional Signals.** Beginning in the mid-1800s, Hg accumulation in lake sediments of the study lakes has increased by about  $3.6 \pm 1.2$  times from that of preindustrial-era values. To 3.4 As previously noted, the rate of accumulation is dependent on spatial differences in the atmospheric Hg loading to these lakes (which is linked to latitude and longitude), the sediment focusing (preferential deposition of fine-grained sediments by wave and current action) in each lake, and the overall propensity for catchment-sourced Hg to be deposited to the lake. Once deposited, Hg signals are well preserved and remineralization and resuspension events are unlikely in these deeper lakes. For these reasons, we feel that these dated lake sediments should sufficiently record temporal Hg deposition without local anthropogenic Hg contamination and be suitable to reconstruct background Hg dynamics through time using Hg stable isotope ratios. Signals are using Hg dynamics through time using Hg stable isotope ratios.

Collectively, the lakes sampled represent four remote regions of North America, and within each region, the resulting Hg isotopic composition exhibits strong positive correlation among isotope values (Pearson's  $r=0.83,\,0.74,\,$  and 0.78, p<0.001 for all, for Figure 1 top to bottom, respectively) but with large regional differences. The coastal lakes of southeastern Alaska and Newfoundland are lower in  $\delta^{202}$ Hg

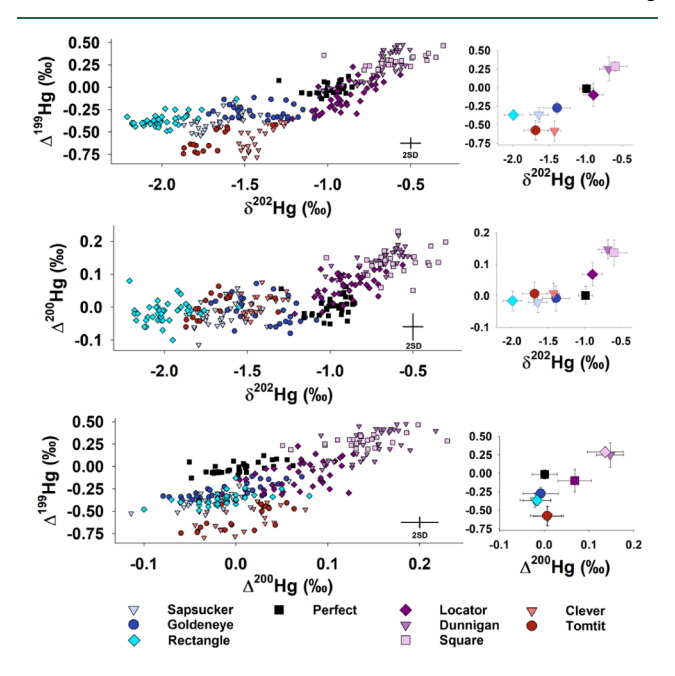


Figure 1. Mercury isotope composition of the individual sediment core intervals (left; error bars reflect  $\pm 2$  SD of IAEA SL1) and averaged core values (right; error bars reflect  $\pm 1$  SD) for each lake where base color (blue, black, purple, and red) is used to delineate region (Southeastern Alaska, Arctic Alaska, Minnesota, and Newfoundland, respectively) and shades and shapes used to further differentiate sites. The top and middle sections plot  $\delta^{202}{\rm Hg}$  (MDF) versus  $\Delta^{199}{\rm Hg}$  (odd-MIF) and  $\Delta^{200}{\rm Hg}$  (even-MIF), respectively, while the bottom plots  $\Delta^{200}{\rm Hg}$  (even-MIF) versus  $\Delta^{199}{\rm Hg}$  (odd-MIF). Values may be found in Table S2, and information regarding the strength of these relationships may be found in Table S4 and S5.

(ranging: -2.21 to -1.05 and -1.87 to -1.25%, respectively) when compared to the Alaskan arctic (ranging: -1.29 to -0.85%) and northern Minnesota lakes (ranging: -1.21 to -0.30%). Similarly,  $\Delta^{199}$ Hg values of the coastal lakes of southeastern Alaska and Newfoundland are lower (ranging: -0.53 to -0.11 and -0.79 to -0.38%, respectively) than the Alaskan arctic (ranging: -0.12 to 0.12%) and northern Minnesota lakes (ranging: -0.35 to 0.47%). Given the strong coherence in isotopic signatures among lakes within each region, the regional differences are likely attributable to geographic contrasts in the isotopic composition of direct atmospheric inputs to these lakes, whereas local watershed or in-lake effects represent a secondary and relatively minor control in the signals measured.

The positive trend between the  $\delta^{202}$ Hg and  $\Delta^{199}$ Hg (Figure 1 top) is likely due to controls on isotopic distribution at both the source and process level. The dominant mechanism that produces nonzero values of  $\Delta^{199}$ Hg in lake sediments, where Hg is dominantly inorganic Hg, is photochemical reduction<sup>23,38,50</sup> which is empirically assessed by comparing the slope of  $\Delta^{199}$ Hg:  $\Delta^{201}$ Hg (here, 1.14  $\pm$  0.04;  $r^2$  = 0.95—Figure S5) from the sediments to the slope for photochemical reduction derived in laboratory settings (0.85-1.46; depending on system conditions). 20,23,50,51 This work suggests that ecosystem conditions (dissolved oxygen, pH, dissolved organic carbon quality, and functional groups binding Hg) can leave residue Hg, which can then bind to sediment, with either  $+\Delta^{199}$ Hg (hydroxyl-bound Hg, sulfur-bound Hg pH 7—anoxic conditions) or  $-\Delta^{199} Hg$  (high DOC-induced abiotic reduction, N-bound Hg, S-bound Hg acidic pH in anoxia, and pH—oxic conditions) values. <sup>27,50,52</sup> Unfortunately, the DOC ligand-Hg binding structure is rarely known in ecosystem-relative conditions and thus we cannot expand upon this topic further. Our study lakes are circumneutral (pH between 6 and 8.5) and dominantly oxic in the photic region (periodic suboxia at the sediment interface where photochemical reactions are less likely), thus we do not expect water-column Hg reduction processes to be the dominant driver for the observed ranges in  $\delta^{202}$ Hg and  $\Delta^{199}$ Hg. Additionally, the lakes with the highest and lowest  $\Delta^{199}$ Hg values (Locator/Dunnigan and Clever/ Tomtit) also had the highest dissolved organic carbon (DOC) concentrations  $(6.6-13.7 \text{ mg L}^{-1})$  of the study sites.<sup>7</sup> DOC was not significantly related to the  $\Delta^{199}$ Hg: $\delta^{202}$ Hg slopes (Pearson's r = 0.55; p = 0.12), indicating that the changes in  $\delta^{202}$ Hg are not the result of changed photochemical reduction rates in the atmosphere, contrary to previous findings. 13,53 Thus, the variance in sediment  $\Delta^{199}$ Hg values must be dominated by the relative source contributions (directly and through the watershed) as are the  $\delta^{202} \mathrm{Hg}$  values when compared to global endmembers.<sup>20</sup> However, we cannot discount in situ processes that might produce changes in  $\delta^{202}$ Hg values but not  $\Delta^{199}$ Hg, thus resulting in inconsistent  $\Delta^{199}$ Hg: $\delta^{202}$ Hg slopes from lake to lake.

Organic carbon in sediments is either the byproduct of autochthonous carbon from primary production or allochthonous terrestrial organic matter. Hg isotope characterization of in-lake primary production is limited, but consistently has positive  $\Delta^{199} {\rm Hg}^{55}$  values in planktonic matter, whereas Hg delivered from the terrestrial environment as particulate matter consistently has negative  $\Delta^{199} {\rm Hg}$  values. Thus, at nonzero  $\Delta^{199} {\rm Hg}$  values, the relative influence of these two carbon and Hg delivery pathways can be compared in sediments. The ratio of Hg to organic carbon in sediments was negatively associated

with  $\Delta^{199}$ Hg (Pearson's r=-0.72, p=0.03), likely reflecting the relative importance of Hg captured by and delivered from the terrestrial system ( $-\Delta^{199}$ Hg) compared to Hg captured by in-lake biological production ( $+\Delta^{199}$ Hg). Further supporting this, lakes with larger catchment to lake area ratios, a surrogate for the relative influence of the terrestrial sources, tended to have more Hg captured by and delivered from the terrestrial system ( $-\Delta^{199}$ Hg; not statistically significant, Pearson's r=-0.50).

Traditionally,  $\Delta^{200}$ Hg has been used to estimate the relative proportions of gaseous elemental Hg (GEM) from the atmosphere ( $-\Delta^{200}$ Hg) and precipitation-delivered Hg ( $+\Delta^{200}$ Hg). Based upon empirical observations,  $^{28,29,33,35,36,59}$  the proportion of atmospheric Hg delivered by these two pathways can be compared in sediments and biological specimens. To date, one laboratory study has linked  $\Delta^{200}$ Hg formation as well as shifts in  $\delta^{202}$ Hg and  $\Delta^{199}$ Hg, to halogen oxidation. While processes that produce  $\Delta^{200}$ Hg also produce subtle changes to  $\delta^{202}$ Hg and  $\Delta^{199}$ Hg values, the relative magnitude of this effect for the latter isotope systems is negligible. For this reason, we consider  $\Delta^{200}$ Hg as independent of processes controlling  $\delta^{202}$ Hg and  $\Delta^{199}$ Hg and therefore use it as a relative source tracer for the delivery pathway (GEM deposition versus wet deposition) of atmospheric Hg.

While processes that alter  $\Delta^{200}$ Hg are different than processes that produce the larger observable fractionations of  $\delta^{202}$ Hg and  $\Delta^{199}$ Hg, the three isotope signals are all positively associated. This indicates that differences in  $\delta^{202} {\rm Hg}$ ,  $\Delta^{199} {\rm Hg}$ , and  $\Delta^{200}$ Hg among the lakes must be primarily controlled by Hg sources and altered only little by in-lake processes such as resuspension, methylation, demethylation, and remineralization, each which produce changes to  $\delta^{202}$ Hg and  $\Delta^{199}$ Hg values. <sup>20–22,38,49,60–63</sup> To better understand the effect of atmospherically delivered Hg, we compared sediment isotopic composition to Hg deposition from the Mercury Deposition Network (MDN) stations nearest the study sites over the last decade. Both wet Hg deposition and the overall proportion of Hg from precipitation to a given lake were significantly and positively correlated with  $\Delta^{200}$ Hg (Pearson's r = 0.85 and 0.65, respectively; Table S4) as well as  $\delta^{202}$ Hg (Pearson's r = 0.75and 0.64, respectively); correlations of wet Hg deposition with  $\Delta^{199}$ Hg were not significant (Pearson's r = 0.61 and 0.42, respectively).

Trends in Time. The time period represented in the lakesediment records began between 900 and 1800 with most beginning prior to the 15th century (Table S2).7-9,16,40 Changes in Hg stable isotope values were asynchronous among the lakes over relatively short time intervals (decadal scale) and did not convincingly record any preindustrial Hg releases such as that associated with New World gold and silver extraction during the Spanish colonial period (1400–1600s; Table S2).8 Over broad time scales, there was coherence in the change in isotope shifts (Figure 2), particularly following the global industrialization beginning around 1800. However, the magnitude of response was variable among lakes and linked to the relative effect of atmospheric Hg deposition, directly or indirectly, to a lake. Also, short-lived Hg releases, such as the California gold (and silver) rush,8 also fail to register in these isotopic records, possibly because the signal was local or regional rather than of global significance. Similarly, there is little evidence for isotopic shifts associated with recent declines in global Hg emissions<sup>64-66</sup> possibly because associated reductions in Hg deposition have occurred predominately in

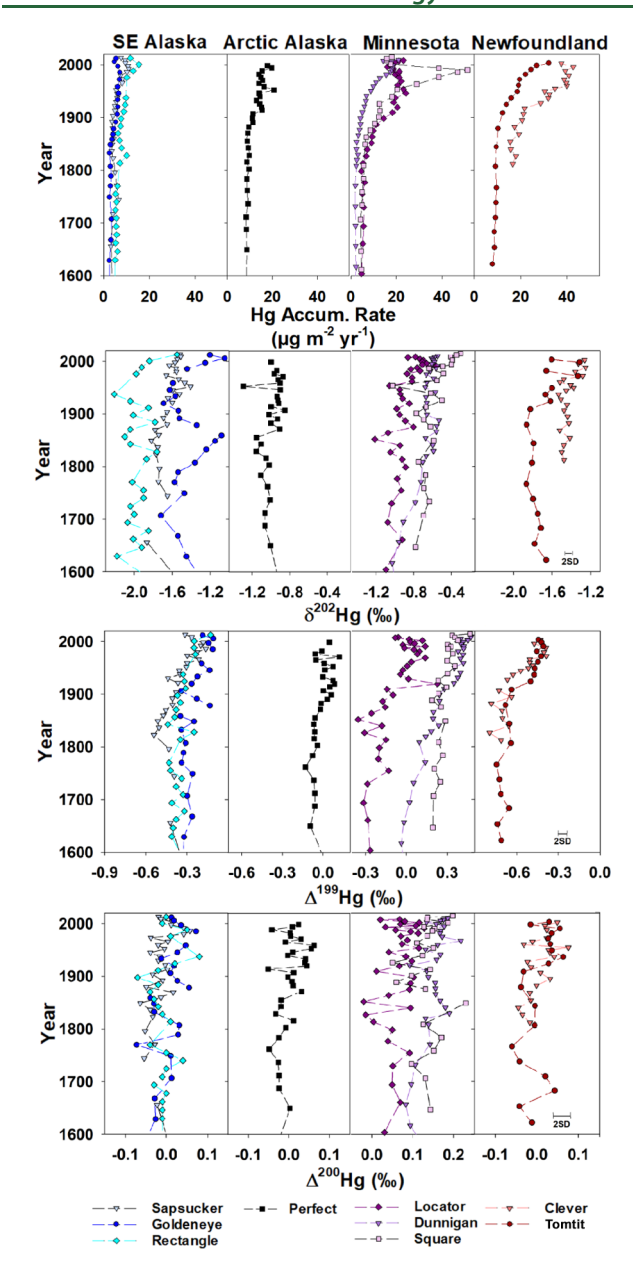


Figure 2. Mercury isotope composition and accumulation rates of the dated sediment cores where base color (blue, black, purple, and red) is used to delineate region (Southeastern Alaska, Arctic Alaska, Minnesota, and Newfoundland, respectively) and shades and shapes used to further differentiate sites. Error bars reflect ±2 SD of IAEA SL1.

urban and industrialized regions and are thus absent in sediment records from remote lakes.  $^{7,67}$ 

 $\delta^{202}$ Hg and  $\Delta^{199}$ Hg in Newfoundland cores are among the most negative sediments reported in the literature. Mechanistically, these negative values could be attributable to the strong effect of terrestrial-sourced Hg, except that the magnitude of negative  $\delta^{202}$ Hg and  $\Delta^{199}$ Hg are beyond previously measured terrestrial-bound Hg in North America, particularly prior to the onset of industrialization. While it is likely that terrestrial-bound Hg has shifted like sediments through time, we hypothesize that an underlying co-variable may partially explain why sediments from these near-coastal sites are so negative. We suggest that enhanced oxidation of GEM by halogens (Br and CI) in near-coastal environments,

possibly via sea spray, may be contributing to Hg deposition in these regions.  $^{68,69}$  Direct halogen oxidation or oxidation mediated by sunlight may be responsible for the deposition of reactive mercury with a decreased  $\Delta^{199} \rm Hg$  value  $^{26}$  in our coastal study lakes as well as to preindustrial coastal sediments reported elsewhere.  $^{70}$  Although this mechanism has not been directly measured, halogen oxidation of GEM in the Arctic has also demonstrated the large potential for negative  $\Delta^{199} \rm Hg$  formation.  $^{71,72}$ 

Hg in sea water exhibits positive  $\Delta^{199}$ Hg,<sup>73</sup> so we do not suspect oceanic-sourced Hg to be responsible for this decreased  $\Delta^{199}$ Hg. Finally, the chloride content in lake water of our study sites was inversely and strongly related to  $\Delta^{199}$ Hg (Pearson's r = -0.82, p = 0.01), further supporting the notion that oceanic sea spray is affecting these near-coastal environments.

The  $\delta^{202}$ Hg,  $\Delta^{199}$ Hg, and  $\Delta^{200}$ Hg values of Hg depositing to these lakes since about 1820 have increased, contemporaneous with the onset of industrialization. However, each lake responded to a different degree, and understanding the drivers for the increases in the isotopic values is important to translating these results broadly. At the lake level, the magnitude of these changes in  $\delta^{202}$ Hg,  $\Delta^{199}$ Hg, and  $\Delta^{200}$ Hg from preindustrial to present day is positively associated with the increase in Hg accumulation over this same time period (the Hg flux ratio; Table S4—Pearson's r = 0.69, 0.78, and 0.92, respectively). Moreover, the Hg flux ratio is positively related to overall contribution of wet deposition Hg to each lake, calculated previously  $^{7-9,40}$  (Pearson's r = 0.75). For this reason, we suspect that the shift in the overall global signal of atmospheric Hg is responsible for the increases in Hg isotope composition in each lake, while the magnitude of response is dependent on both the proportion of Hg sourced from the atmosphere, specifically from precipitation, and the overall net increase in Hg deposited through time.

Extending These Results to Models. The Hg isotope values in sediments from remote lakes have responded uniformly in direction to a change in the global Hg isotope composition, with increases in  $\delta^{202}$ Hg,  $\Delta^{199}$ Hg, and  $\Delta^{200}$ Hg. Therefore, we can estimate the shifts in the isotope values of the global pool through time, if our study lakes are representative of North American lakes at large. To do so, we have standardized temporal changes in the Hg isotope composition as the difference from the average background (1600–1775) and calculated kernel smoothed 50th percentiles over the sliding time window across all lakes (Figure 3). After 1820, all three isotope systems begin to increase markedly at linear rates of 0.013 and 0.0014% decade<sup>-1</sup> for  $\Delta^{199}$ Hg and  $\Delta^{200}$ Hg, respectively, and exponentially for  $\delta^{202}$ Hg. Although not quantified in this manner, increases in  $\delta^{202}$ Hg,  $\Delta^{199}$ Hg, and  $\Delta^{200}$ Hg values have been reported in other studies examining Hg deposition of regions largely remote from direct anthropogenic Hg releases. 18,39,49,53,61,74,75

Such information is needed when modeling global changes in Hg composition and understanding the change in atmospheric Hg isotope values of Hg depositing to lakes between preanthropogenic and present conditions. Previous modeling of global emission inventories has similarly predicted that due to the large releases of anthropogenic Hg sources, the global atmospheric  $\delta^{202}$ Hg values have increased ( $\sim$ 0.4‰) over time (since 1820). However, these studies predicted  $\Delta^{199}$ Hg and  $\Delta^{200}$ Hg to change little and remain slightly negative and near-zero, respectively. Here, we found that a

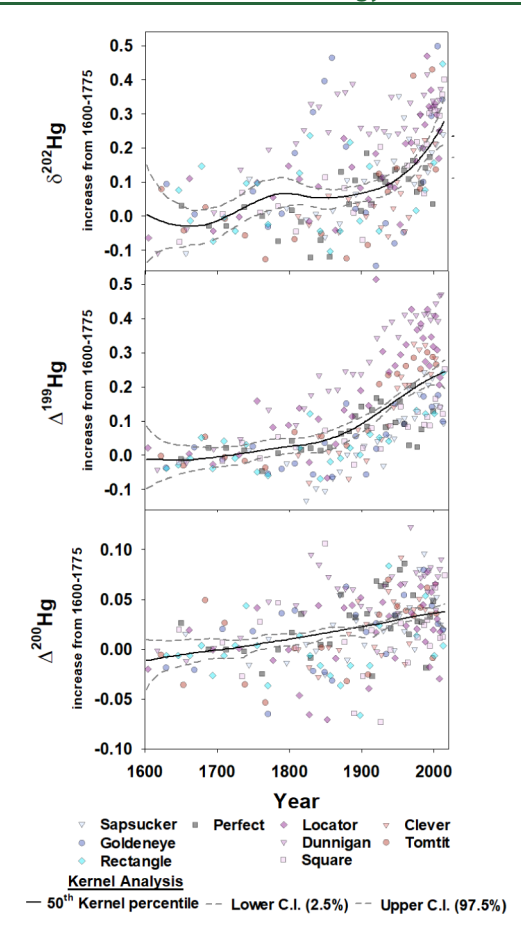


Figure 3. Relative changes in the mercury isotope composition of sediment cores over time. Points represent the difference between isotopic values for each core interval and their respective preindustrial baselines (here defined as 1600-1775) divided by the averaged isotope value for that specific core. The black line then traces the Kernel smoothed trend for the entire data set, and the gray dotted lines trace the 2.5 and 97.5 percentiles, to show the combined trend across North America. Note that the analytical variability of  $\Delta^{200}$ Hg is 0.04% at a given data point, and thus while the endpoints of the kernel regression are statistically distinguishable, caution is advised when interpretation of the overall trend.

steady rise in Hg emissions with these modeled isotopic signatures could explain, in part, the consistent increases in  $\delta^{202}$ Hg,  $\Delta^{199}$ Hg, and  $\Delta^{200}$ Hg observed in those lake sediments exhibiting strongly negative preindustrial  $\Delta^{199} Hg$  and  $\Delta^{200} Hg$ baseline values. However, this modeling does not adequately explain isotopic trends in our Minnesota lakes, which have high preindustrial  $\Delta^{199}$ Hg and  $\Delta^{200}$ Hg values that also continue to increase through time. We suggest that these Minnesota trends are linked to an increasing proportion of precipitationdelivered Hg that has become elevated in Hg from regional anthropogenic emissions that experience an aqueous photochemical reduction and thus increased  $\Delta^{199}$ Hg values prior to deposition. However, due to this relatively near-field effect,  $\Delta^{200}$ Hg values are not as strongly affected because Hg from these regional emissions do not reach the upper atmosphere to form positive  $\Delta^{200}$ Hg values prior to depositing to the lake surface. Thus,  $\Delta^{200}$ Hg values measured in lake sediments continue to capture the continental-scale effects while  $\Delta^{199}$ Hg values show a small degree of local enhancement relative to the continental signal. Such a scenario would also explain why

increases in  $\delta^{202}$ Hg values have outpaced the MDF predicted from photochemical reactions.

Our sediment records from remote North American lakes demonstrate a consistent increase in  $\delta^{202}$ Hg,  $\Delta^{199}$ Hg, and  $\Delta^{200}$ Hg values (0.22  $\pm$  0.07, 0.2  $\pm$  0.03, and 0.03  $\pm$  0.01‰, respectively, for 1775–2015) over a geographically widespread area since industrialization. The mercury budget of these lakes is dominated by atmospheric inputs and thus likely reflects how the global pool of atmospheric Hg (gaseous oxidized Hg, gaseous elemental Hg, particle-bound Hg) has responded to changes in anthropogenic emissions through time. These coherent shifts in Hg isotope values following the onset of industrialization, when paired with historical increases in Hg deposition, provide a more complete picture of human alteration of the global mercury cycle—one that is similar to the Suess effect of anthropogenic CO<sub>2</sub> emissions observed in carbon isotope ratios.

# ASSOCIATED CONTENT

# Supporting Information

The Supporting Information is available free of charge at https://pubs.acs.org/doi/10.1021/acs.est.0c00579.

All raw data of the site characteristics, Hg isotope values, associated quality assurance, and statistical evaluations. Site map; smoothed kernel analysis on the Z-scores; smoothed LOWESS analysis on enrichment factors; smoothed LOWESS analysis on the Z-scores; odd-MIF and even-MIF regression lines; site physicochemical characteristics; chemical constituents measured on the sediment intervals; quality assurance and quality controls; Pearson's analysis table comparing averaged 1600–1775 sediments and averaged 1990—present day; Pearson's analysis table comparing Hg isotope values within sites and over similar publications (PDF)

# AUTHOR INFORMATION

# **Corresponding Author**

Ryan F. Lepak — Environmental Chemistry and Technology Program, University of Wisconsin-Madison, Madison, Wisconsin 53706, United States; U.S. Geological Survey, Upper Midwest Water Science Center, USGS Mercury Research Laboratory, Middleton, Wisconsin 53562, United States; U.S. Environmental Protection Agency Office of Research and Development, Center for Computational Toxicology and Exposure, Great Lakes Toxicology and Ecology Division, Duluth, Minnesota 55804, United States; orcid.org/0000-0003-2806-1895; Email: rlepak@wisc.edu

# **Authors**

Sarah E. Janssen — U.S. Geological Survey, Upper Midwest Water Science Center, USGS Mercury Research Laboratory, Middleton, Wisconsin 53562, United States; ⊚ orcid.org/ 0000-0003-4432-3154

Daniel R. Engstrom — St. Croix Watershed Research Station, Science Museum of Minnesota, Marine on St. Croix, Minnesota 55047, United States; oorcid.org/0000-0002-8066-029X

David P. Krabbenhoft — U.S. Goological Survey, Upper Midwest Water Science Center, USGS Mercury Research Laboratory, Middleton, Wisconsin 53562, United States; orcid.org/0000-0003-1964-5020

- Michael T. Tate U.S. Geological Survey, Upper Midwest Water Science Center, USGS Mercury Research Laboratory, Middleton, Wisconsin 53562, United States
- Runsheng Yin State Key Laboratory of Ore Deposit Geochemistry, Institute of Geochemistry, Chinese Academy of Sciences, Guiyang, Guizhou 550081, China; orcid.org/ 0000-0001-9631-5303
- William F. Fitzgerald Department of Marine Sciences, University of Connecticut, Groton, Connecticut 06340, United States; © orcid.org/0000-0003-3592-1662
- Sonia A. Nagorski Department of Natural Sciences, University of Alaska Southeast, Juneau, Alaska 99801, United States
- James P. Hurley Environmental Chemistry and Technology Program, University of Wisconsin-Madison, Madison, Wisconsin 53706, United States; University of Wisconsin Aquatic Sciences Center, Madison, Wisconsin 53706, United States; orcid.org/0000-0003-4430-5319

Complete contact information is available at: https://pubs.acs.org/10.1021/acs.est.0c00579

# **Author Contributions**

R.F.L., D.R.E., D.P.K., Y.R., S.E.J., S.A.N., and J.P.H. designed the study. R.F.L., D.R.E., and J.P.H. wrote this manuscript. D.R.E., S.A.N., and W.F.F. provided samples. R.F.L., S.E.J., M.T.T., R.Y., and D.R.E. provided substantial analytical support. S.E.J., M.T.T., R.Y. S.A.N., W.F.F., and D.R.E. provided editorial comments.

#### Notes

The authors declare no competing financial interest.

## ACKNOWLEDGMENTS

This work was supported by the U.S. Geological Survey Toxic Substances Hydrology Program. The views expressed in this paper represent the views solely of the authors of the U.S. Environmental Protection Agency but do represent the views or position of the U.S. Geological Survey. Any use of trade, firm, or product names is for descriptive purposes only and does not imply endorsement by the U.S. Government. Partial graduate student support was provided by the Wisconsin Alumni Research Foundation through the University of Wisconsin-Madison Graduate School (award no. MSN165161) and the University of Wisconsin Water Resources Institute through a USGS-NIWR fellowship (award no. MSN197848). Postdoctoral support was provided by the National Science Foundation Postdoctoral Fellowships for Research in Biology—Collection Program 2018 (award no. 1812211). Support for the lake studies and coring was provided to W.F.F. and D.R.E through the U.S.EPA-STAR (Science to Achieve Results) Program (Grants R829796 and 91643401), the NSF Office of Polar Programs (Grant 9908895) and to S.A.N and D.R.E. through the National Park Service PNW CESU Task Agreement (P14AC01393). We thank Ed Swain, Bruce Monson, Carl Lamborg, and Prentiss Balcom for assistance in collecting the sediment cores used in this study, and Dale Robertson who contributed a volunteer peer review of this work and its findings. Data collected for this study are available in Lepak and Janssen  $(2020)^{42}$ 

## **■** REFERENCES

(1) Selin, N. E. Global biogeochemical cycling of mercury: a review. *Annu. Rev. Environ. Resour.* **2009**, *34*, 43–63.

- (2) Hsu-Kim, H.; Kucharzyk, K. H.; Zhang, T.; Deshusses, M. A. Mechanisms regulating mercury bioavailability for methylating microorganisms in the aquatic environment: a critical review. *Environ. Sci. Technol.* **2013**, *47*, 2441–2456.
- (3) Wiener, J. G.; Sandheinrich, M. B.; Bhavsar, S. P.; Bohr, J. R.; Evers, D. C.; Monson, B. A.; Schrank, C. S. Toxicological significance of mercury in yellow perch in the Laurentian Great Lakes region. *Environ. Pollut.* **2012**, *161*, 350–357.
- (4) Trasande, L.; Landrigan, P. J.; Schechter, C. Public health and economic consequences of methyl mercury toxicity to the developing brain. *Environ. Health Perspect.* **2005**, *113*, 590–596.
- (5) Evers, D. C.; Savoy, L. J.; DeSorbo, C. R.; Yates, D. E.; Hanson, W.; Taylor, K. M.; Siegel, L. S.; Cooley, J. H.; Bank, M. S.; Major, A. Adverse effects from environmental mercury loads on breeding common loons. *Ecotoxicology* **2008**, *17*, 69–81.
- (6) Drevnick, P. E.; Cooke, C. A.; Barraza, D.; Blais, J. M.; Coale, K. H.; Cumming, B. F.; Curtis, C. J.; Das, B.; Donahue, W. F.; Eagles-Smith, C. A. Spatiotemporal patterns of mercury accumulation in lake sediments of western North America. *Sci. Total Environ.* **2016**, *568*, 1157–1170.
- (7) Engstrom, D. R.; Balogh, S. J.; Swain, E. B. History of mercury inputs to Minnesota lakes: influences of watershed disturbance and localized atmospheric deposition. *Limnol. Oceanogr.* **2007**, *52*, 2467–2483.
- (8) Engstrom, D. R.; Fitzgerald, W. F.; Cooke, C. A.; Lamborg, C. H.; Drevnick, P. E.; Swain, E. B.; Balogh, S. J.; Balcom, P. H. Atmospheric Hg emissions from preindustrial gold and silver extraction in the Americas: A reevaluation from lake-sediment archives. *Environ. Sci. Technol.* **2014**, *48*, 6533–6543.
- (9) Engstrom, D. R.; Swain, E. B. Recent declines in atmospheric mercury deposition in the upper Midwest. *Environ. Sci. Technol.* **1997**, 31, 960–967.
- (10) Sun, R.; Jiskra, M.; Amos, H. M.; Zhang, Y.; Sunderland, E. M.; Sonke, J. E. Modelling the mercury stable isotope distribution of Earth surface reservoirs: Implications for global Hg cycling. *Geochim. Cosmochim. Acta* **2019**, 246, 156–173.
- (11) Sun, R.; Streets, D. G.; Horowitz, H. M.; Amos, H. M.; Liu, G.; Perrot, V.; Toutain, J.-P.; Hintelmann, H.; Sunderland, E. M.; Sonke, J. E. Historical (1850–2010) mercury stable isotope inventory from anthropogenic sources to the atmosphere. *Elem. Sci. Anth.* **2016**, *4*, No. 000091.
- (12) Patterson, C. C. The Reduction of Orders of Magnitude Errors in Lead Analyses of Biological Materials and Natural Waters by Evaluating and Controlling the Extent and Sources of Industrial Lead Contamination Introduced During Sample Collecting, Handling, and Analysis. In Accuracy in Trace Analysis: Sampling, Sample Handling, and Analysis; US Department of Commerce, National Bureau of Standards, 1976; Vol. 321.
- (13) Cooke, C. A.; Hintelmann, H.; Ague, J. J.; Burger, R.; Biester, H.; Sachs, J. P.; Engstrom, D. R. Use and legacy of mercury in the Andes. *Environ. Sci. Technol.* **2013**, *47*, 4181–4188.
- (14) Appleby, P. Chronostratigraphic Techniques in Recent Sediments. In *Tracking Environmental Change Using Lake Sediments*; Springer, 2002; pp 171–203.
- (15) Bandara, S.; Froese, D.; St. Louis, V. L.; Cooke, C.; Calmels, F. Post-depositional mercury mobility in a permafrost peatland from central Yukon, Canada. *ACS Earth Space Chem.* **2019**, No. 00010.
- (16) Biester, H.; Bindler, R.; Martinez-Cortizas, A.; Engstrom, D. R. Modeling the past atmospheric deposition of mercury using natural archives. *Environ. Sci. Technol.* **2007**, *41*, 4851–4860.
- (17) Cooke, C. A.; Martínez-Cortizas, A.; Bindler, R.; Gustin, M. S. Environmental archives of atmospheric Hg deposition—A review. *Sci. Total Environ.* **2020**, *709*, No. 134800.
- (18) Zdanowicz, C. M.; Krümmel, E.; Poulain, A.; Yumvihoze, E.; Chen, J.; Štrok, M.; Scheer, M.; Hintelmann, H. Historical variations of mercury stable isotope ratios in Arctic glacier firn and ice cores. *Global Biogeochem. Cycles* **2016**, *30*, 1324–1347.

- (19) Blum, J. D.; Bergquist, B. A. Reporting of variations in the natural isotopic composition of mercury. *Anal. Bioanal. Chem.* **2007**, 388, 353–359.
- (20) Blum, J. D.; Sherman, L. S.; Johnson, M. W. Mercury isotopes in earth and environmental sciences. *Annu. Rev. Earth Planet. Sci.* **2014**, *42*, 249–269.
- (21) Jiskra, M.; Wiederhold, J. G.; Bourdon, B.; Kretzschmar, R. Solution speciation controls mercury isotope fractionation of Hg (II) sorption to goethite. *Environ. Sci. Technol.* **2012**, *46*, 6654–6662.
- (22) Janssen, S. E.; Schaefer, J. K.; Barkay, T.; Reinfelder, J. R. Fractionation of mercury stable isotopes during microbial methylmercury production by iron-and sulfate-reducing bacteria. *Environ. Sci. Technol.* **2016**, *50*, 8077–8083.
- (23) Bergquist, B. A.; Blum, J. D. Mass-dependent and-independent fractionation of Hg isotopes by photoreduction in aquatic systems. *Science* **2007**, *318*, 417–420.
- (24) Tsui, M. T.-K.; Blum, J. D.; Kwon, S. Y. Review of stable mercury isotopes in ecology and biogeochemistry. *Sci. Total Environ.* **2019**, No. 135386.
- (25) Chandan, P.; Ghosh, S.; Bergquist, B. A. Mercury isotope fractionation during aqueous photoreduction of monomethylmercury in the presence of dissolved organic matter. *Environ. Sci. Technol.* **2014**, *49*, 259–267.
- (26) Sun, G.; Sommar, J.; Feng, X.; Lin, C.-J.; Ge, M.; Wang, W.; Yin, R.; Fu, X.; Shang, L. Mass-dependent and-independent fractionation of mercury isotope during gas-phase oxidation of elemental mercury vapor by atomic Cl and Br. *Environ. Sci. Technol.* **2016**, *50*, 9232–9241.
- (27) Wiederhold, J. G.; Cramer, C. J.; Daniel, K.; Infante, I.; Bourdon, B.; Kretzschmar, R. Equilibrium mercury isotope fractionation between dissolved Hg (II) species and thiol-bound Hg. *Environ. Sci. Technol.* **2010**, *44*, 4191–4197.
- (28) Chen, J.; Hintelmann, H.; Feng, X.; Dimock, B. Unusual fractionation of both odd and even mercury isotopes in precipitation from Peterborough, ON, Canada. *Geochim. Cosmochim. Acta* **2012**, 90. 33–46.
- (29) Chen, J.; Hintelmann, H.; Zheng, W.; Feng, X.; Cai, H.; Wang, Z.; Yuan, S.; Wang, Z. Isotopic evidence for distinct sources of mercury in lake waters and sediments. *Chem. Geol.* **2016**, 426, 33–44.
- (30) Mead, C.; Lyons, J. R.; Johnson, T. M.; Anbar, A. D. Unique Hg stable isotope signatures of compact fluorescent lamp-sourced Hg. *Environ. Sci. Technol.* **2013**, *47*, 2542–2547.
- (31) Blum, J. D.; Johnson, M. W. Recent developments in mercury stable isotope analysis. *Rev. Mineral. Geochem.* **2017**, *82*, 733–757.
- (32) Demers, J. D.; Blum, J. D.; Zak, D. R. Mercury isotopes in a forested ecosystem: Implications for air-surface exchange dynamics and the global mercury cycle. *Global Biogeochem. Cycles* **2013**, 27, 222–238.
- (33) Demers, J. D.; Sherman, L. S.; Blum, J. D.; Marsik, F. J.; Dvonch, J. T. Coupling atmospheric mercury isotope ratios and meteorology to identify sources of mercury impacting a coastal urban-industrial region near Pensacola, Florida, USA. *Global Biogeochem. Cycles* **2015**, *29*, 1689–1705.
- (34) Fu, X.; Marusczak, N.; Wang, X.; Gheusi, F. O.; Sonke, J. E. Isotopic composition of gaseous elemental mercury in the free troposphere of the Pic du Midi Observatory, France. *Environ. Sci. Technol.* **2016**, *50*, 5641–5650.
- (35) Rolison, J.; Landing, W.; Luke, W.; Cohen, M.; Salters, V. Isotopic composition of species-specific atmospheric Hg in a coastal environment. *Chem. Geol.* **2013**, *336*, 37–49.
- (36) Sherman, L. S.; Blum, J. D.; Dvonch, J. T.; Gratz, L. E.; Landis, M. S. The use of Pb, Sr, and Hg isotopes in Great Lakes precipitation as a tool for pollution source attribution. *Sci. Total Environ.* **2015**, *S02*, 362–374
- (37) Lepak, R. F.; Janssen, S. E.; Yin, R.; Krabbenhoft, D. P.; Ogorek, J. M.; DeWild, J. F.; Tate, M. T.; Holsen, T. M.; Hurley, J. P. Factors Affecting Mercury Stable Isotopic Distribution in Piscivorous Fish of the Laurentian Great Lakes. *Environ. Sci. Technol.* **2018**, *52*, 2768–2776.

- (38) Lepak, R. F.; Yin, R.; Krabbenhoft, D. P.; Ogorek, J. M.; DeWild, J. F.; Holsen, T. M.; Hurley, J. P. Use of stable isotope signatures to determine mercury sources in the Great Lakes. *Environ. Sci. Technol. Lett.* **2015**, *2*, 335–341.
- (39) Enrico, M.; Le Roux, Gl.; Heimbürger, L.-E.; Van Beek, P.; Souhaut, M.; Chmeleff, Jr.; Sonke, J. E. Holocene atmospheric mercury levels reconstructed from peat bog mercury stable isotopes. *Environ. Sci. Technol.* **2017**, *51*, 5899–5906.
- (40) Fitzgerald, W. F.; Engstrom, D. R.; Lamborg, C. H.; Tseng, C.-M.; Balcom, P. H.; Hammerschmidt, C. R. Modern and historic atmospheric mercury fluxes in northern Alaska: Global sources and Arctic depletion. *Environ. Sci. Technol.* **2005**, *39*, 557–568.
- (41) Nagorski, S. A.; Engstrom, D. R.; Krabbenhoft, D. P.; Lepak, R. F.; Fitzgerald, W. F. *Historical Trends in Mercury Deposition as Recorded in Lake Cores Near Glacier Bay National Park and Preserve, Alaska*; Natural Resource Report, NPS/SEAN/NRR—2019/1928; National Park Service: Fort Collins, Colorado, 2019.
- (42) Lepak, R. F.; Janssen; Sarah, E. Data Release for Resolving Atmospheric Mercury Loading and Source Trends from Isotopic Records in Remote North American Lakes; U.S. Geological Survey, 2020 DOI: 10.5066/P9ISRL9C.
- (43) Swain, E. B.; Engstrom, D. R.; Brigham, M. E.; Henning, T. A.; Brezonik, P. L. Increasing rates of atmospheric mercury deposition in midcontinental North America. *Science* **1992**, *257*, 784–787.
- (44) Eakins, J. A.; Morrison, R. A new procedure for the determination of lead-210 in lake and marine sediments. *Int. J. Appl. Radiat. Isot.* **1978**, 29, 531–536.
- (45) EPA, U. Method 1631, Revision E: Mercury in Water by Oxidation, Purge and Trap, and Cold Vapor Atomic Fluorescence Spectrometry; US Environmental Protection Agency: Washington, DC, 2002.
- (46) Yin, R.; Krabbenhoft, D. P.; Bergquist, B. A.; Zheng, W.; Lepak, R. F.; Hurley, J. P. Effects of mercury and thallium concentrations on high precision determination of mercury isotopic composition by Neptune Plus multiple collector inductively coupled plasma mass spectrometry. *J. Anal. At. Spectrom.* **2016**, *31*, 2060–2068.
- (47) Janssen, S.; Lepak, R.; Tate, M.; Ogorek, J.; DeWild, J.; Babiarz, C.; Hurley, J.; Krabbenhoft, D. Rapid pre-concentration of mercury in solids and water for isotopic analysis. *Anal. Chim. Acta* **2018**, No. 95.
- (48) Krissansen-Totton, J.; Buick, R.; Catling, D. C. A statistical analysis of the carbon isotope record from the Archean to Phanerozoic and implications for the rise of oxygen. *Am. J. Sci.* **2015**, *315*, 275–316.
- (49) Yin, R.; Lepak, R. F.; Krabbenhoft, D. P.; Hurley, J. P. Sedimentary records of mercury stable isotopes in Lake Michigan. *Elem. Sci. Anth.* **2016**, *4*, No. 000086.
- (50) Motta, L. C.; Kritee, K.; Blum, J. D.; Tsz-Ki Tsui, M.; Reinfelder, J. R. Mercury Isotope Fractionation during the Photochemical Reduction of Hg (II) Coordinated with Organic Ligands. *J. Phys. Chem. A* **2020**, *124*, 2842–2853.
- (51) Zheng, W.; Hintelmann, H. Isotope fractionation of mercury during its photochemical reduction by low-molecular-weight organic compounds. *J. Phys. Chem. A* **2010**, *114*, 4246–4253.
- (52) Zheng, W.; Hintelmann, H. Nuclear field shift effect in isotope fractionation of mercury during abiotic reduction in the absence of light. *J. Phys. Chem. A* **2010**, *114*, 4238–4245.
- (53) Kurz, A. Y.; Blum, J. D.; Washburn, S. J.; Baskaran, M. Changes in the mercury isotopic composition of sediments from a remote alpine lake in Wyoming, USA. *Sci. Total Environ.* **2019**, *669*, 973–982.
- (54) Binford, M. W.; Brenner, M. Dilution of 210Pb by organic sedimentation in lakes of different trophic states, and application to studies of sediment-water interactions 1. *Limnol. Oceanogr.* **1986**, *31*, 584–595.
- (55) Perrot, V.; Epov, V. N.; Pastukhov, M. V.; Grebenshchikova, V. I.; Zouiten, C.; Sonke, J. E.; Husted, S.; Donard, O. F.; Amouroux, D. Tracing sources and bioaccumulation of mercury in fish of Lake Baikal— Angara River using Hg isotopic composition. *Environ. Sci. Technol.* **2010**, *44*, 8030–8037.

- (56) Kwon, S. Y.; Blum, J. D.; Nadelhoffer, K. J.; Dvonch, J. T.; Tsui, M. T.-K. Isotopic study of mercury sources and transfer between a freshwater lake and adjacent forest food web. *Sci. Total Environ.* **2015**, 532, 220–229.
- (57) Tsui, M. T.-K.; Blum, J. D.; Finlay, J. C.; Balogh, S. J.; Nollet, Y. H.; Palen, W. J.; Power, M. E. Variation in terrestrial and aquatic sources of methylmercury in stream predators as revealed by stable mercury isotopes. *Environ. Sci. Technol.* **2014**, *48*, 10128–10135.
- (58) Washburn, S. J.; Blum, J. D.; Kurz, A. Y.; Pizzuto, J. E. Spatial and temporal variation in the isotopic composition of mercury in the South River, VA. *Chem. Geol.* **2018**, 494, 96–108.
- (59) Cai, H.; Chen, J. Mass-independent fractionation of even mercury isotopes. *Sci. Bull.* **2016**, *61*, 116–124.
- (60) Jiskra, M.; Wiederhold, J. G.; Skyllberg, U.; Kronberg, R.-M.; Kretzschmar, R. Source tracing of natural organic matter bound mercury in boreal forest runoff with mercury stable isotopes. *Environ. Sci.: Processes Impacts* **2017**, *19*, 1235–1248.
- (61) Yin, R.; Feng, X.; Hurley, J. P.; Krabbenhoft, D. P.; Lepak, R. F.; Kang, S.; Yang, H.; Li, X. Historical records of mercury stable isotopes in sediments of Tibetan lakes. *Sci. Rep.* **2016**, *6*, No. 23332.
- (62) Yin, R.; Guo, Z.; Hu, L.; Liu, W.; Hurley, J. P.; Lepak, R. F.; Lin, T.; Feng, X.; Li, X. Mercury Inputs to Chinese Marginal Seas—Impact of Industrialization and Development of China. *J. Geophys. Res.: Oceans* **2018**, *123*, 5599–5611.
- (63) Zheng, W.; Demers, J. D.; Lu, X.; Bergquist, B. A.; Anbar, A. D.; Blum, J. D.; Gu, B. Mercury Stable Isotope Fractionation during Abiotic Dark Oxidation in the Presence of Thiols and Natural Organic Matter. *Environ. Sci. Technol.* **2018**, *53*, 1853–1862.
- (64) Zhang, Y.; Jacob, D. J.; Horowitz, H. M.; Chen, L.; Amos, H. M.; Krabbenhoft, D. P.; Slemr, F.; Louis, V. L. S.; Sunderland, E. M. Observed decrease in atmospheric mercury explained by global decline in anthropogenic emissions. *Proc. Natl. Acad. Sci. U.S.A.* **2016**, *113*, 526–531.
- (65) Horowitz, H. M.; Jacob, D. J.; Amos, H. M.; Streets, D. G.; Sunderland, E. M. Historical mercury releases from commercial products: Global environmental implications. *Environ. Sci. Technol.* **2014**, *48*, 10242–10250.
- (66) Schuster, P. F.; Krabbenhoft, D. P.; Naftz, D. L.; Cecil, L. D.; Olson, M. L.; Dewild, J. F.; Susong, D. D.; Green, J. R.; Abbott, M. L. Atmospheric mercury deposition during the last 270 years: a glacial ice core record of natural and anthropogenic sources. *Environ. Sci. Technol.* 2002, 36, 2303–2310.
- (67) Fitzgerald, W. F.; Engstrom, D. R.; Hammerschmidt, C. R.; Lamborg, C. H.; Balcom, P. H.; Lima-Braun, A. L.; Bothner, M. H.; Reddy, C. M. Global and local sources of mercury deposition in coastal New England reconstructed from a multiproxy, high-resolution, estuarine sediment record. *Environ. Sci. Technol.* **2018**, 52, 7614–7620.
- (68) Obrist, D.; Tas, E.; Peleg, M.; Matveev, V.; Faïn, X.; Asaf, D.; Luria, M. Bromine-induced oxidation of mercury in the mid-latitude atmosphere. *Nat. Geosci.* **2011**, *4*, 22.
- (69) Timonen, H.; Ambrose, J.; Jaffe, D. Oxidation of elemental Hg in anthropogenic and marine airmasses. *Atmos. Chem. Phys.* **2013**, *13*, 2827–2836.
- (70) Gray, J. E.; Pribil, M. J.; Van Metre, P. C.; Borrok, D. M.; Thapalia, A., Identification of contamination in a lake sediment core using Hg and Pb isotopic compositions, Lake Ballinger, Washington, USA. *Appl. Geochem.* **2013**, *29*, 1–12.
- (71) Douglas, T. A.; Blum, J. D. Mercury isotopes reveal atmospheric gaseous mercury deposition directly to the Arctic coastal snowpack. *Environ. Sci. Technol. Lett.* **2019**, *6*, 235–242.
- (72) Sherman, L. S.; Blum, J. D.; Johnson, K. P.; Keeler, G. J.; Barres, J. A.; Douglas, T. A. Mass-independent fractionation of mercury isotopes in Arctic snow driven by sunlight. *Nat. Geosci.* **2010**, *3*, 173.
- (73) Štrok, M.; Baya, P. A.; Hintelmann, H. The mercury isotope composition of Arctic coastal seawater. C. R. Geosci. 2015, 347, 368–376.
- (74) Mil-Homens, M.; Blum, J.; Canário, J.; Caetano, M.; Costa, A. M.; Lebreiro, S. M.; Trancoso, M.; Richter, T.; de Stigter, H.;

- Johnson, M. Tracing anthropogenic Hg and Pb input using stable Hg and Pb isotope ratios in sediments of the central Portuguese Margin. *Chem. Geol.* **2013**, *336*, *62*–71.
- (75) Das, R.; Bizimis, M.; Wilson, A. M. Tracing mercury seawater vs. atmospheric inputs in a pristine SE USA salt marsh system: mercury isotope evidence. *Chem. Geol.* **2013**, *336*, 50–61.

#### NOTE ADDED AFTER ASAP PUBLICATION

This paper was published ASAP on July 10, 2020, with an error in Figure 2. The corrected version was reposted on July 16, 2020.